Bioorganic & Medicinal Chemistry 25 (2017) 1860–1866

Contents lists available at ScienceDirect

Bioorganic & Medicinal Chemistry

journal homepage: www.elsevier.com/locate/bmc

An epigenetic modifier induces production of (10′*S*)-verruculide B, an inhibitor of protein tyrosine phosphatases by *Phoma* sp. nov. LG0217, a fungal endophyte of *Parkinsonia microphylla*

Juliana R. Gubiani [a,b], E.M. Kithsiri Wijeratne [a], Taoda Shi [c], Angela R. Araujo [b], A. Elizabeth Arnold [d], Eli Chapman [c], A.A. Leslie Gunatilaka [a,*]

[a] *Natural Products Center, School of Natural Resources and the Environment, College of Agriculture and Life Sciences, University of Arizona, 250 E. Valencia Road, Tucson, AZ 85706, United States*
[b] *NuBBE – Núcleo de Bioensaios, Biossíntese e Ecofisiologia de Produtos Naturais, Departamento de Química Orgânica, Instituto de Química, UNESP, Universidade Estadual Paulista, Araraquara, SP 14800-900, Brazil*
[c] *Department of Pharmacology and Toxicology, College of Pharmacy, University of Arizona, Tucson, AZ 85721, United States*
[d] *School of Plant Sciences, College of Agriculture and Life Sciences, University of Arizona, Tucson, AZ 85721, United States*

ARTICLE INFO

Article history:
Received 23 November 2016
Revised 30 January 2017
Accepted 31 January 2017
Available online 3 February 2017

Keywords:
Epigenetic
Phoma sp. nov. LG0217
Histone deacetylase inhibitor
(10′*S*)-verruculide B
Protein tyrosine phosphatases

ABSTRACT

Incorporation of the histone deacetylase (HDAC) inhibitor, suberoylanilide hydroxamic acid (SAHA), to a culture broth of the endophytic fungus *Phoma* sp. nov. LG0217 isolated from *Parkinsonia microphylla* changed its metabolite profile and resulted in the production of (10′*S*)-verruculide B (**1**), vermistatin (**2**) and dihydrovermistatin (**3**). When cultured in the absence of the epigenetic modifier, it produced a new metabolite, (*S*,*Z*)-5-(3′,4′-dihydroxybutyldiene)-3-propylfuran-2(5H)-one (**4**) together with nafuredin (**5**). The structure of **4** was elucidated by spectroscopic analyses and its absolute configuration was determined by application of the modified Mosher's ester method. The absolute structure of (10′*S*)-verruculide B was determined as 5-[(10′*S*,2′*E*,6′*E*)-10′,11′-dihydroxy-3′,7′,11′-trimethyldodeca-2′,6′-dien-1′-yl]-(3*R*)-6,8-dihydroxy-3-methylisochroman-1-one (**1**) with the help of CD and NOE data. Compound **1** inhibited the activity of protein tyrosine phosphatases (PTPs) 1B (PTP1B), Src homology 2-containing PTP 1 (SHP1) and *T*-cell PTP (TCPTP) with IC_{50} values of 13.7 ± 3.4, 8.8 ± 0.6, and 16.6 ± 3.8 μM, respectively. Significance of these activities and observed modest selectivity of **1** for SHP1 over PTP1B and TCPTP is discussed.

© 2017 Elsevier Ltd. All rights reserved.

1. Introduction

Endophytic fungi are a group of endosymbiotic microorganisms that inhabit healthy plant tissues with no apparent pathogenic effects on their hosts.[1] Recent studies have shown that endophytic fungi are prolific producers of bioactive and/or novel secondary metabolites.[2] However, when cultured utilizing traditional fermentation techniques, fungi often express only a subset of biosynthetic genes which encode for their secondary metabolite production.[3] Realization of this has recently led to the discovery of strategies to activate these silent biosynthetic gene clusters in fungi including the use of epigenetic modifiers to activate silent biosynthetic pathways,[4] and simulation of natural gene cluster activating conditions by biotic (co-cultivation),[5] and abiotic (elicitation by chemical and physical means)[6] methods. Among these, incorporation of small-molecule modifiers into fungal culture media to manipulate epigenetic regulation of gene transcription has received considerable attention primarily focusing on inhibitors of histone deacetylase (HDAC),[7] DNA methyltransferase (DNMT)[8] and the proteasome.[9]

To investigate the effect of incorporation of the HDAC inhibitor, suberoylanilide hydroxamic acid (SAHA), on production of secondary metabolites, we screened a small collection of endophytic fungi by culturing them in potato dextrose broth (PDB) medium with SAHA (100, 250, and 500 μM) and without this epigenetic modifier, and then by analyzing the resulting EtOAc extracts by HPLC. Among those investigated, *Phoma* sp. nov. LG0217, a fungal endophyte of *Parkinsonia microphylla* (foothills paloverde, family: Fabaceae), showed a significant difference in HPLC profiles of the extracts derived from a culture grown with SAHA (500 μM) and the control culture (Fig. 1) whereas no such effect was observed

* Corresponding author.
E-mail address: leslieg1@email.arizona.edu (A.A.L. Gunatilaka).

http://dx.doi.org/10.1016/j.bmc.2017.01.048
0968-0896/© 2017 Elsevier Ltd. All rights reserved.

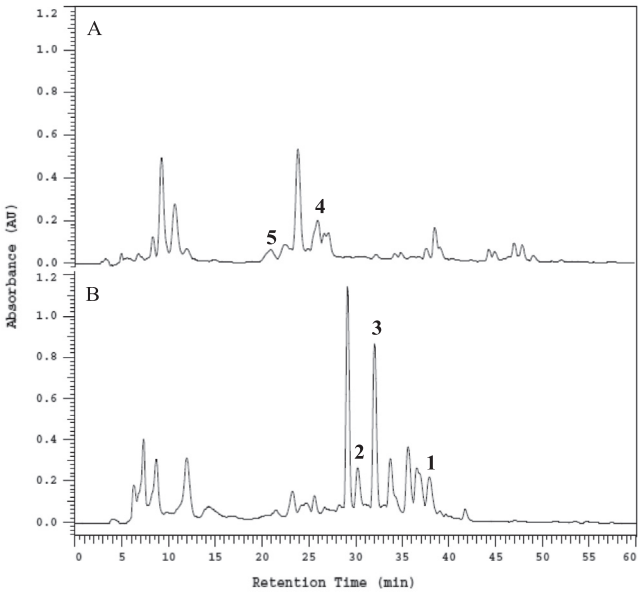

Fig. 1. (**A**) HPLC profiles of the EtOAc extracts of *Phoma* sp. nov. LG0217 cultured in PDB and (**B**) PDB containing 500 μM SAHA detected by UV absorption at 280 nm. Note: Those metabolites indicated above HPLC peaks have been isolated and characterized (see Fig. 2), but the remaining peaks in HPLC traces were found to be complex inseparable mixtures and/or undergo decomposition during isolation.

at SAHA concentrations of 100 and 200 μM. Chemical investigation of the culture broth treated with SAHA led to the isolation of (10′*S*)-verruculide B (**1**),[10] vermistatin (**2**)[12] and dihydrovermistatin (**3**)[13] whereas the control culture broth afforded a new metabolite, (*S*,*Z*)-5-(3′,4′-dihydroxybutylidene)-3-propylfuran-2(5*H*)-one (**4**) together with nafuredin (**5**)[14] (Fig. 2). Vermistatin (**2**) has been reported to act as an elastase inhibitor,[15] phytotoxin on various banana cultivars,[16] RNA synthesis inhibitor in Ehrlich ascites carcinoma,[17] P-388 leukemia,[17] weakly cytotoxic to KB tumor cell lines,[18] and an inhibitor of α-glucosidase.[19] Reported biological activities of nafuredin (**5**) include selective inhibition of helminth complex I and inhibition of NADH-fumarate reductase (NFRD) of *Ascaris suum* (pig roundworm) at nM concentrations.[14a] Verruculide B has been evaluated previously for its inhibitory activity against protein tyrosine phosphatase (PTP) 1B (PTP1B) and was found to exhibit 40% inhibition at 23.1 μM.[11] Therefore, it was of interest to evaluate **1** for its activity against other PTPs. Herein we report the isolation of **1**–**5**, structure elucidation and determination of absolute stereochemistry of **1** and **4** and evaluation of **1** for inhibition of PTPs including PTP1B, T-cell PTP (TCPTP),

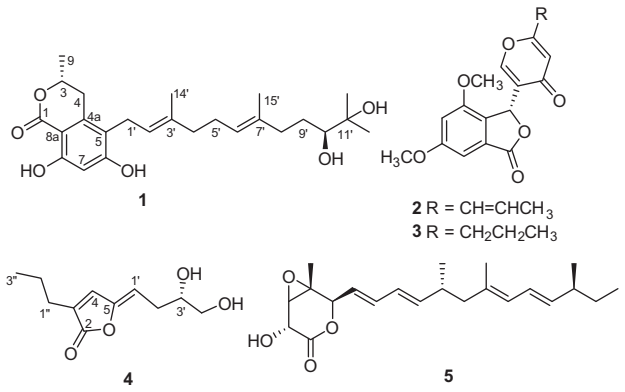

Fig. 2. Structures of metabolites **1**–**5** isolated from *Phoma* sp. nov. LG0217.

PTP non-receptor type 3 (PTPN3), PTP non-receptor type 5 (PTPN5), PTP non-receptor type 7 (PTPN7), Src homology 2-containing PTP 1 (SHP1), and Src homology 2-containing PTP 2 (SHP2).[20]

2. Results and discussion

HPLC analyses of EtOAc soluble portions of MeOH/$CHCl_3$ extracts derived from freeze-dried cultures of *Phoma* sp. nov. LG0217 cultured in PDB and PDB + SAHA (500 μM) differed markedly in their metabolite profiles (Fig. 1). Thus, each extract was fractionated separately resulting in the isolation of metabolites **1**–**3** from the PDB + SAHA culture broth extract and **4**–**5** from the PDB culture broth (control) extract. The spectroscopic (UV, IR, MS, ^{1}H and ^{13}C NMR) data for **1** were similar to those reported for verruculide B,[11] except for the $[\alpha]_D$ data (+2.0 for **1**; −45.2 for verruculide B[11]). Although the absolute configuration of one of the two chiral centers (C-3) of verruculide B has been determined as *R* by the application of CD spectroscopy and comparison with the related 6,8-dihydroxy-3-methylisochroman-1-one [(*R*)-6-hydroxymellein], application of the modified Mosher's ester method to define the absolute configuration of the remaining chiral center (C-10′) located in the side chain has been reported to be unsuccessful.[11] Based on differences in $[\alpha]_D$ data for **1** and verruculide B (see above), it was essential to determine the absolute configurations of both chiral centers (C-3 and C-10′) of **1**. The absolute configuration of C-3 of **1** was established from the Cotton effect observed in its CD spectrum. The negative Cotton effect ascribed to the K-absorption band at 270 nm in the CD spectrum confirmed the *R* absolute configuration at C-3 of **1** (see Supplementary Fig. 12).[21] The availability of a hydroxy group attached to the carbon atom (C-11′) adjacent to the side chain chiral center (C-10′) of **1** made it possible to apply *in situ* dimolybdenum CD method developed for vicinal diols by Snatzke and Frelek[22] for the determination of the absolute configuration of this chiral center. The positive Cotton effect at 305 nm observed in the $Mo_2(OAc)_4$-induced CD spectrum of **1** (Fig. 3) suggested the absolute configuration of C-10′ to be *S*.[22] Thus, absolute structure of **1** was determined as

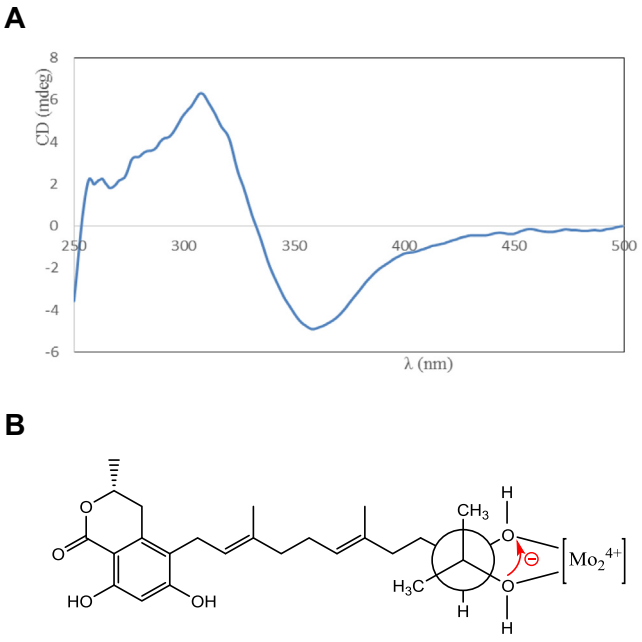

Fig. 3. (**A**) CD spectrum of **1** with dimolybdinum tetraacetate in DMSO solution (after subtracting the inherent CD spectrum of **1**), and (**B**) preferred conformation of the diol in the chiral Mo-complex.

5-[(10′*S*,2′*E*,6′*E*)-10′,11′-dihydroxy-3′,7′,11′-trimethyldodeca-2′,6′-dien-1′-yl]-(3*R*)-6,8-dihydroxy-3-methylisochroman-1-one [(10′*S*)-verruculide B].

Metabolite **4**, obtained as a yellow oil, was determined to have the molecular formula $C_{11}H_{16}O_4$ by a combination of HRFABMS and NMR data, indicating four degrees of unsaturation. Analysis of ^{1}H, ^{13}C and HSQC NMR data revealed that **4** contained a primary methyl [δ_H 0.94 (t, J = 7.0 Hz); δ_C 13.7], four methylenes of which one was oxygenated [δ_H 3.68 (dd, J = 11.0, 3.0 Hz), 3.49 (dd, J = 11.0, 7.0 Hz); δ_C 66.3], one oxymethine [δ_H 3.85 (m); δ_C 71.3], five sp^2 carbons, two of which were protonated [δ_H 6.97 (s); δ_C 136.7 and δ_H 5.25 (t, J = 8.0 Hz); δ_C 109.2] and one was a lactone carbonyl (δ_C 170.5). Since two double bonds and carbonyl group accounted for three degrees of unsaturation, **4** should be monocyclic. The presence of two spin systems, $CH_3CH_2CH_2$— and $HOCH_2CH(OH)$—CH_2CH═, in **4** were evident from its ^{1}H–^{1}H COSY spectrum (Fig. 4). The connectivities of these two spin systems and the remaining structural (two trisubstituted olefins and lactone) moieties in **4** were determined by the analysis of its HMBC correlations (Fig. 4). In the HMBC spectrum, the correlations between terminal CH_2 protons [H_2-1″ (δ_H 2.31)] of the $CH_3CH_2CH_2$— spin system and lactone carbonyl carbon (δ_C 170.5), olefinic carbon [C-3 (δ_C 134.2)] and protonated olefinic carbon [C-4 (δ_C 136.7)] were observed, which established the connectivity of C-1″ with C-3, lactone carbonyl (C-2) with C-3, and C-3 with C-4. The HMBC correlations of the olefinic proton [H-1′ (δ_H 5.25)] of the $HOCH_2CH(OH)$–CH_2CH═ spin system with C-5 (δ_C 149.8) and C-4 (δ_C 136.7) established the connectivity between C-5 and C-1′. Taken together these data suggested that the lactone carbonyl should be linked to C-5 *via* an oxygen atom to form a five membered ring. The proton H-4 showed long-range coupling with H-1′ (J = 1.5 Hz) suggesting that both these protons are on the same side of the molecule. The absolute configuration of the chiral carbon (C-3′) of **4** was determined by the application of the modified Mosher's ester method.[23] Reaction of **4** with (*R*)- and (*S*)-α-methoxy-α-trifluoromethylphenylacetyl chloride (MTPA-Cl) afforded (*S*)- and (*R*)- MTPA bisesters **4a** and **4b**, respectively. Analysis of $\Delta\delta$ ($\delta_S - \delta_R$) values of these Mosher's esters confirmed the *S* absolute stereochemistry for C-3′ of **4** (see Fig. 5 and Supplementary Fig. 13). Thus, the absolute structure of **4** was determined as (*S*,*Z*)-5-(3′,4′-dihydroxybutylidene)-3-propylfuran-2(5*H*)-one [(*S*,*Z*)-7,8-dihydroxy-2-propyl-octa-2,4-dien-4-olide]. Metabolites **2**, **3** and **5** were identified as vermistatin,[12] dihydrovermistatin,[13] and nafuredin,[14] respectively by comparison of their spectroscopic (^{1}H and ^{13}C NMR) and $[\alpha]_D$ data with those reported.

PTPs are key regulatory enzymes that dephosphorylate phosphotyrosine residues and are critical regulators of signal transduction under normal and pathological conditions. In conjunction with protein tyrosine kinases (PTKs), they regulate the reversible phosphorylation of tyrosine residues in proteins. Thus, PTPs control fundamental physiological processes such as cell growth and differentiation, cell cycle, metabolism, immune responses and cytoskeletal function. In addition, interfering with the delicate balance between counteracting PTKs, PTPs are involved in the development of numerous inherited and acquired human diseases such as autoimmunity, diabetes and cancer.[24] When evaluated

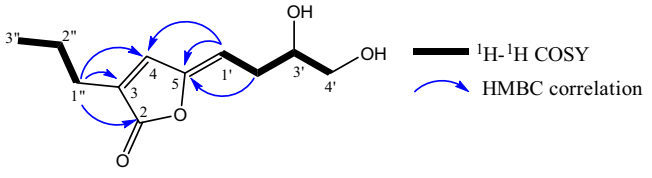

Fig. 4. ^{1}H–^{1}H COSY and selected HMBC correlations for **4**.

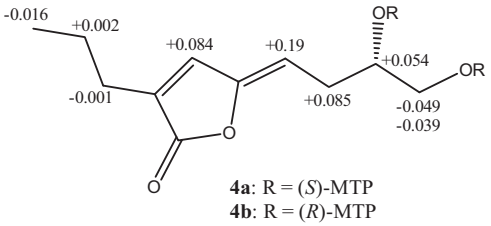

Fig. 5. $\Delta\delta_H$ values [($\Delta\delta$ in ppm) = $\delta_S - \delta_R$] obtained for (*S*)- and (*R*)-bis MTP esters (**4a** and **4b**, respectively) of (*S*,*Z*)-5-(3′,4′-dihydroxybutylidene)-3-propylfuran-2(5*H*)-one (**4**) in d_5-pyridine.

for inhibition of a small panel of protein tyrosine phosphatases PTP1B, TCPTP, PTPN3, PTPN5, PTPN7, SHP1, and SHP2 in our screening assays, (10′*S*)-verruculide B (**1**) showed significant inhibitory activity for SHP1 and moderate activity for PTP1B and TCPTP (Fig. 6). It was found that **1** inhibited SHP1 with an IC_{50} = 8.8 ± 0.6 μM and showed modest selectivity for SHP1 versus PTP1B (1.6-fold) and TCPTP (1.9-fold). PTP1B is a negative regulator of insulin and leptin signaling pathway and as such is predicted to be an attractive target for metabolic diseases such as type 2 diabetes and obesity.[25]

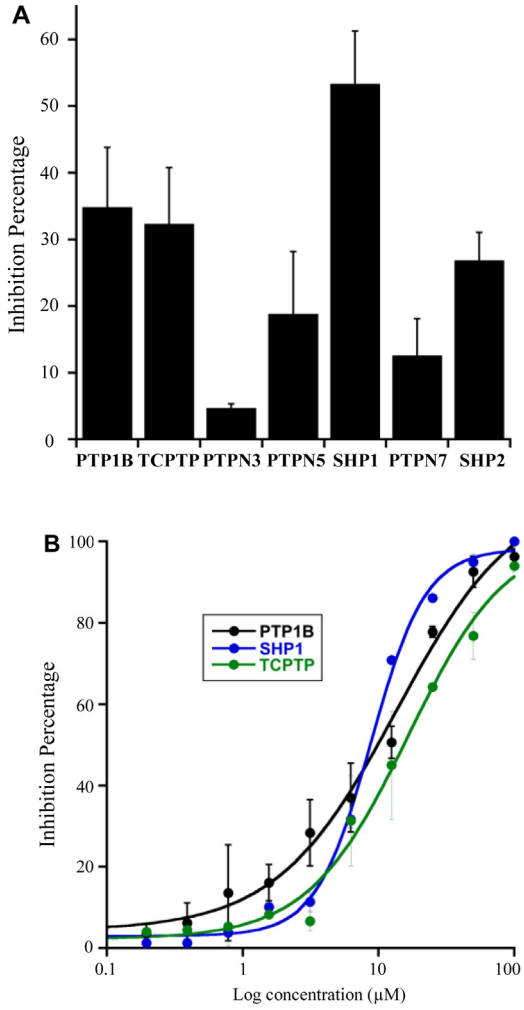

Fig. 6. Inhibition of PTPs by (10′*S*)-verruculide B (**1**). (**A**) Percentage inhibition of a panel of protein tyrosine phosphatases by **1**. (**B**) Dose-response curves of **1** for inhibition of PTP1B, TCPTP, and SHP1.

Compromised TCPTP function has been associated with autoimmune diseases like type 1 diabetes and Crohn's disease,[26] and obesity related metabolic disorders through antagonism of insulin and leptin signaling.[27] Conversely, SHP1 has been linked to a number of cancer correlated phenotypes with a complex relationship. For instance, it is known to antagonize growth related tyrosine kinases,[28] and to promote responsiveness and antitumor functions of natural killer (NK) cells.[29] However, SHP1 activity has also been linked to metastasis via the epithelial-mesenchymal transition.[30] Although **1** had moderate to weak inhibitory activity for PTPs tested with modest selectivity for SHP1, it offers an interesting lead molecule that could be optimized through strategies involving epigenetic culture manipulation and/or medicinal chemistry.

3. Experimental

3.1. General experimental procedures

Optical rotations were measured with a JASCO Dip-370 digital polarimeter using $CHCl_3$ as solvent. UV spectra were recorded on a Shimadzu UV-1601 UV–vis spectrophotometer. IR spectra for KBr disks were recorded on a Shimadzu FTIR-8300 spectrometer. NMR spectra were recorded in $CDCl_3$ with a Bruker Avance III 400 spectrometer at 400 MHz for ^1H NMR and 100 MHz for ^{13}C NMR, using residual $CHCl_3$ as internal reference. High-resolution MS were recorded on Bruker LCQ-Fleet spectrometer. CD spectra were recorded in MeOH or DMSO on a Jasco 810 spectrometer at 25 °C, using a quartz cell with 1 mm optical path length. Whatman LRP-2 was used for reversed-phase column chromatography. Analytical and preparative thin-layer chromatography (TLC) was carried out on RP-18 F_{254S} Aluminum-backed TLC plates (Merck) and compounds were visualized with short-wavelength UV and by spraying with anisaldehyde-sulfuric acid spray reagent and heating until the spots appeared. Analytical HPLC was performed on a Hitachi instrument equipped with L-6200A intelligent pump, L-4500 diode array detector, and P-6000 interface utilizing Hitachi Model D-7000 chromatography data station software using a RP column (Phenomenex 5 μm, C-18, 4.6 × 250 mm). Injections (10 μL) were made with AS-4000 intelligent auto sampler. Preparative HPLC was performed on a Waters Delta Prep 400 preparative chromatography system equipped with Waters 996 photodiode array detector and a Water Prep LC controller utilizing Empower Pro software and using a RP column (Phenomenex Luna 5 μm, C18, 10 × 250 mm). Dimolybdenum tetracetate was purchased from Sigma-Aldrich. DMSO was purchased from Sigma-Aldrich and dried with 4 Å molecular sieves. cDNA constructs and primers were purchased from DNAsu and Integrated DNA Technologies (IDT), respectively. A Techne Prime Thermocycler was used for all polymerase chain reactions (PCR). The Microfluidizer used was purchased from Microfluidics. Talon Cobalt Resin was purchased from Clontech. A BioTek Synergy 2 plate reader was used to measure absorbance of 96-well plates, data were recorded and processed using Gen 5 1.11 software. Graphs were generated with Kaleidagraph 4.5. Culture dishes were purchased from Greiner Bio-One. Gradient SDS PAGE (4–20%) gels were purchased from Invitrogen. Life Technologies gel boxes were used for protein staining.

3.2. Fungal isolation and identification

In October 2011, branches of *Parkinsonia microphylla* (foothills palo verde) were collected from a semi-urban area in Tucson, Arizona. Healthy leaves and photosynthetic stems of these branches were washed in tap water and cut into ca. 2.0 mm^2 segments that were surface-sterilized by agitating sequentially in 95% EtOH for 30 s, 0.5% NaOCl for 2 min, and 70% EtOH for 2 min.[31] Tissue segments were surface-dried under sterile conditions and then placed individually onto 2% malt extract agar in 1.5 mL microcentrifuge tubes. Tubes were sealed with Parafilm and incubated under ambient light/dark condition for one year. Emergent fungi were isolated into pure culture on 2% MEA, vouchered in sterile water, and deposited as living vouchers at the Robert L. Gilbertson Mycological Herbarium at the University of Arizona. One fungus of interest was used for the present study: isolate LG0217, which has been deposited at the Robert L. Gilbertson Mycological Herbarium with accession number LG0217. Total genomic DNA was extracted from fresh mycelium[32] and the internal transcribed spacers and 5.8S gene (ITSrDNA) was amplified and sequenced by PCR.[32] The ITSrDNA sequence was compared against the GenBank database using BLAST.[33] The top BLAST matches were to unnamed fungi isolated from other desert plants,[32] with several species of *Phoma* and allied taxa that were studied by Davey and Currah.[34] We therefore downloaded the alignment published by Davey and Currah,[34] trimmed it to include closely related taxa that were readily alignable with LG0217, and integrated two representative sequences.[32] The resulting alignment consisted of species of *Phoma, Ascochyta, Didymella,* and *Westerdykella* (outgroup), for a total of 24 ingroup taxa and one outgroup taxon. The data set was aligned automatically using MUSCLE (http://www.ebi.ac.uk/Tools/msa/muscle/) with default parameters and verified by eye prior to analysis. The data set was analyzed using maximum likelihood in PAUP 4.0a147[35] followed by a bootstrap analysis with 100 replicates. The strain was placed with strong support in the *Phoma/Ascochyta/Didymella* complex identified by Davey and Currah.[34] This strain was thus designated as *Phoma* sp. nov. LG0217 (Pleosporaceae, Pleosporales, Dothideomycetes, Ascomycota), pending morphological description.

3.3. Cultivation and isolation of metabolites

A seed culture of *Phoma* sp. nov. LG0217 grown on PDA for two weeks was used for inoculation. Mycelia were scraped out, mixed with sterile water, and filtered through a 100 μm filter to separate spores from the mycelia. Absorbance of the spore solution was measured (at 600 nm) and adjusted to between 0.8 and 1.0. This spore solution was used to inoculate 4 × 2.0 L Erlenmeyer flasks, each holding 1.0 L of the medium (PDB) containing 500 μM of SAHA and 5 × 2.0 L Erlenmeyer flasks, each holding 1.0 L of the medium (PDB) and incubated at 160 rpm and 28 °C. The glucose level in the medium was monitored using glucose strips (URISCAN glucose strips). On day 14, the strip gave a blue color for the glucose test, indicating the absence of glucose in the medium. After incubation for 14 days at 28 °C, the culture broth was freeze-dried and extracted with MeOH/$CHCl_3$ (1:1, 1.0 L), and the resulting extract was filtered through Whatman No. 1 filter paper. The filtrate was evaporated under reduced pressure and the resulting residue was suspended in H_2O (500 mL) and extracted with EtOAc (3 × 1.0 L). Combined EtOAc extract was evaporated under reduced pressure to afford an orange semisolid from the fungus cultured in PDB containing 500.0 μM of SAHA (1.54 g) and a dark brown semisolid from the control (3.82 g). A portion (1.33 g) of EtOAc extract from the fungus cultured in PDB containing SAHA was chromatographed over a column of C18 (66 g) made up in MeOH/H_2O (1:9) and eluted with MeOH/H_2O (1:9, 270 mL), MeOH/H_2O (2:8, 270 mL), MeOH/H_2O (3:7, 270 mL), MeOH/H_2O (4:6, 270 mL), MeOH/H_2O (1:1, 270 mL), MeOH/H_2O (6:4, 270 mL), MeOH/H_2O (7:3, 270 mL), MeOH/H_2O (8:2, 270 mL), MeOH (270 mL) and finally with $CHCl_3$ (270 mL) to afford 10 fractions [A (32.1 mg), B (14.8 mg), C (13.6 mg), D (47.8 mg), E (50.7 mg), F (28.7 mg), G (29.9 mg), H (17.7 mg), I (562.8 mg) and J (285.3 mg)]. Fraction F (28.7 mg) was purified by preparative HPLC (CH_3CN/H_2O,

35:65, 3.0 mL/min) to give **2** (1.6 mg, t_R = 28.33 min) and **3** (0.8 mg, t_R = 29.73 min). Fraction H (17.7 mg) was purified by preparative HPLC (CH_3CN/H_2O, 55:45, 2.0 mL/min) to give **1** (2.1 mg, t_R = 33.07 min).

The EtOAc extract (3.82 g) from the *Phoma* sp. nov. LG0217 cultured in PDB was partitioned between hexanes and 80% aqueous MeOH. The 80% aqueous MeOH fraction was diluted to 50% aqueous MeOH by addition of water and then extracted with $CHCl_3$. Evaporation of $CHCl_3$ under reduced pressure yielded a dark brown semisolid (450 mg). A large portion (400 mg) of this was chromatographed over a column of silica gel (13.6 g) made up in hexanes/EtOAc (8:2) and eluted with hexanes/EtOAc (8:2, 70 mL), hexanes/EtOAc (7:3, 70 mL), hexanes/EtOAc (6:4, 70 mL), hexanes/EtOAc (1:1, 70 mL), hexanes/EtOAc (4:6, 70 mL), hexanes/EtOAc (3:7, 70 mL), hexanes/EtOAc (2:8, 70 mL), EtOAc (70 mL) and finally with MeOH (70 mL). A total of 95 fractions (5 mL each) were collected and combined on the basis of their TLC patterns to yield 13 fractions [A (58.3 mg), B (13.6 mg), C (5.0 mg), D (27.8 mg), E (2.1 mg), F (19.6 mg), G (12.6 mg), H (24.3 mg), I (9.7 mg), J (20.9 mg), K (13.1 mg), L (27.3 mg) and M (125.7 mg)]. Fraction F (6.7 mg) was purified by preparative HPLC (MeOH/H_2O, 9:1, 3.0 mL/min) to give **5** (3.8 mg, t_R = 10.35 min). Fraction K (13.2 mg) was purified by preparative HPLC (CH_3CN/H_2O, 3:7, 2.5 mL/min) to give **4** (2.9 mg, t_R = 12.93 min).

3.3.1. (10′S)-Verruculide B (*1*)

A yellow amorphous solid, $[\alpha]_D^{25}$ + 2.0 (*c* 0.2, $CHCl_3$); UV (MeOH) λ_{max}/nm (log ε) 311 (3.45), 272 (4.21), 207 (2.32); IR (KBr) ν_{max}/cm^{-1} 3385, 1660, 1615, and 1573, 1485, 1263, 1095; ^{1}H NMR (400 MHz, $CDCl_3$) δ 6.29 (^{1}H, s, H-7), 5.09 (^{1}H, t, *J* = 6.2 Hz, H-6′), 4.95 (^{1}H, t, *J* = 6.0 Hz, H-2′), 4.58 (^{1}H, m, H-3), 3.37 (^{1}H, d, *J* = 10.0 Hz, H-10′), 3.20 (2H, brt, *J* = 4.7 Hz, H_2-1′), 2.95 (^{1}H, dd, *J* = 16.0, 3.0 Hz, Ha-4), 2.68 (^{1}H, dd, *J* = 16.0, 11.5 Hz, Hb-4), 2.14 (^{1}H, m, Ha-8′), 2.11 (2H, dd, *J* = 14.3, 6.9 Hz, H_2-5′), 2.04 (2H, dd, *J* = 14.3, 6.9 Hz, H_2-4′), 2.03 (^{1}H, m, Hb-8′), 1.69 (3H, s, H_3-14′), 1.61 (^{1}H, m, Ha-9′), 1.55 (3H, s, H_3-15′), 1.50 (3H, d, *J* = 6.0 Hz, H_3-9), 1.39 (^{1}H, m, Hb-9′), 1.21 and 1.18 (3H each, s, H_3-12′/13′); ^{13}C NMR (100 MHz, $CDCl_3$) δ 170.4 (C, C-1), 162.8 (C, C-8), 161.9 (C, C-6), 138.6 (C, C-4a), 135.9 (C, C-3′), 134.7 (C, C-7′), 124.4 (CH, C-6′), 122.8 (CH, C-2′), 117.3 (C, C-5), 101.9 (CH, C-7), 101.3 (C, C-8a), 78.1 (C, C-10′), 74.8 (C, C-3), 73.1 (C, C-11′), 38.9 (CH_2, C-4′), 36.4 (CH_2, C-8′), 32.0 (CH_2, C-4), 29.3 (CH_2, C-9′), 26.5 (CH_3, C-12′), 25.2 (CH_2, C-5′), 24.4 (CH_2, C-1′), 23.5 (CH_3, C-13′), 20.9 (CH_3, C-9), 16.2 (CH_3, C-15′), 15.9 (CH_3, C-14′); HRESIMS *m*/*z* 455.2397 $[M + Na]^+$ (calcd for $C_{25}H_{36}NaO_4$, 455.2410).

3.3.2. Vermistatin (*2*)

A white amorphous solid; $[\alpha]_D^{25}$ − 96 (*c* 0.3, $CHCl_3$); ^{1}H and ^{13}C NMR data were consistent with those reported.[12]

3.3.3. Dihydrovermistatin (*3*)

A yellow gum; $[\alpha]_D^{25}$ − 110 (*c* 0.2, $CHCl_3$) [lit[13] − 108 (*c* 0.1, $CHCl_3$)]; ^{1}H NMR data were consistent with those reported.[13]

3.3.4. (S,Z)-5-(3′,4′-Dihydroxybutylidene)-3-propylfuran-2(5H)-one (*4*)

A yellow gum, $[\alpha]_D^{25}$ + 10.9 (*c* 0.28, $CHCl_3$); ^{1}H NMR (400 MHz, $CDCl_3$) δ 6.97 (^{1}H, t, *J* = 1.5 Hz, H-4), 5.25 (^{1}H, t, *J* = 8.0 Hz, H-1′), 3.85 (^{1}H, m, H-3′), 3.68 (^{1}H, dd, *J* = 11.0, 3.0 Hz, Ha-4′), 3.49 (^{1}H, dd, *J* = 11.0, 7.0 Hz, Hb-4′), 2.53 (2H, m, H_2-2′), 2.31 (2H, t, *J* = 7.0 Hz, H_2-1″), 1.58 (2H, qt, *J* = 7.5 Hz, H_2-2″), 0.94 (3H, t, *J* = 7.5 Hz, H_3-3″); ^{13}C NMR (400 MHz, $CDCl_3$) δ 170.5 (C, C-2), 149.8 (C, C-5), 136.7 (CH, C-4), 134.2 (C, C-3), 109.2 (CH, C-1′), 71.3 (CH, C-3′), 66.3 (CH_2, C-4′), 30.1 (CH_2, C-2′), 27.1 (CH_2, C-1″), 20.8 (CH_2, C-2″), 13.7 (CH_3, C-3″); HRESIMS *m*/*z* 213.1087 $[M + H]^+$ (calcd for $C_1{}^1H_{17}O_4$, 213.1126).

3.3.5. Nafuredin (*5*)

A yellow amorphous solid; $[\alpha]_D^{25}$ + 90 (*c* 0.1, $CHCl_3$) [lit[14] + 89.9 (*c* 0.1, $CHCl_3$)]; ^{1}H and ^{13}C NMR data were consistent with those reported.[14]

3.4. Determination of absolute configuration at C-10′ of *1*

According to the published procedure,[22] diol/$Mo_2(OAc)_4$ mixture (ca. 1:1) was subjected to CD measurement of **1** at the concentration of 0.3 mg/mL. The first CD spectrum was recorded immediately after mixing, and its time evolution was monitored with a rate of about one spectrum every 10 min until stationary CD was reached (ca. 30 min after mixing). The inherent CD was subtracted. The observed sign of the diagnostic band at 305 nm in the induced CD spectrum was correlated to the absolute configuration of the *vic*-diol moiety.

3.5. Preparation of (S)- and (R)-MTPA bisesters of *4*

Compound **4** (0.5 mg) was transferred into a clean NMR tube and was dried completely under the vacuum. Deuterated pyridine (0.4 mL) and (*R*)-MTPA-Cl (10.0 μL) was added into the NMR tube immediately under a stream of N_2. The reaction in the NMR tube was monitored by ^{1}H NMR and left at 25 °C for 2 h, to give the (*S*)-MTPA bisester derivative (**4a**) of **4**. ^{1}H NMR data of **4a**: (400 MHz, pyridine-d_5). δ 7.166 (^{1}H, t, *J* = 1.5 Hz, H-4), 5.897 (^{1}H, m, H-3′), 5.336 (^{1}H, t, *J* = 8.0 Hz, H-1′), 5.018 (^{1}H, dd, *J* = 12.3, 3.0 Hz, Ha-4′), 4.659 (^{1}H, dd, *J* = 12.3, 5.5 Hz, Hb-4′), 2.979 (2H, m, H_2-2′), 2.260 (2H, t, *J* = 7.3 Hz, H_2-1″), 1.505 (2H, sextet, *J* = 7.3 Hz, H_2-2″), 0.818 (3H, t, *J* = 7.3 Hz, H_3-3″). In the same manner described for **4a** another portion of **4** (0.5 mg) was reacted in a second NMR tube with (*S*)-MTPA-Cl (10.0 μL) at 25 °C for 2 h using d_5-pyridine (0.4 mL) as solvent, to give the (*R*)-MTPA bisester derivative **4b**. ^{1}H NMR data of **4b**: (400 MHz, pyridine-d_5). δ 7.082 (^{1}H, t, *J* = 1.5 Hz, H-4), 5.843 (^{1}H, m, H-3′), 5.146 (^{1}H, t, *J* = 7.7 Hz, H-1′), 5.057 (^{1}H, dd, *J* = 12.0, 2.5 Hz, Ha-4′), 4.708 (^{1}H, dd, *J* = 12.0, 6.5 Hz, Hb-4′), 2.894 (2H, m, H_2-2′), 2.261 (2H, t, *J* = 7.3 Hz, H_2-1″), 1.503 (2H, sextet, *J* = 7.3 Hz, H_2-2″), 0.834 (3H, t, *J* = 7.3 Hz, H_3-3″).

3.6. Ligation independent cloning of PTP expression constructs

Amplifications via PCR were carried out (5.0 μL 10X Pfx buffer, 1.0 μL forward primer (50.0 μM), 1.0 μL reverse primer (50.0 μM), 1.0 μL template (~20.0 nM) 1 μL dNTPs (10.0 mM), 1.0 μL $MgSO_4$ (50 mM), 39.6 μL of H_2O, and 0.4 μL of Pfx polymerase). All reaction materials were pipetted into a PCR tube on ice with Pfx polymerase added last. Reaction mixtures were then placed in a thermal cycler and heated to 95 °C for 5 min, 55 °C for 45 s, and 68 °C for 6 min for 30 cycles. PCR products were analyzed by 1% agarose gel electrophoresis. Gels were stained with ethidium bromide and then washed with buffer. The gels were then examined by UV trans-illuminator. The PCR products (10.0 μL, 100 ng/μL) were then mixed with pSpeedET vector (10.0 μL, 100.0 ng/μL) for 10 min at 25 °C and used to transform *E. coli* DH5α cells. A single colony was picked and used to inoculate 3.0 mL of Terrific Broth (TB) media. Plasmids were purified via a Qiagen miniprep kit. The correct sequences were confirmed by Sanger sequencing.

3.7. PTP expression and purification

BL21 DE3 *E. coli* cells were transformed with the desired plasmid. A single colony was picked and used to inoculate 10.0 mL of LB media supplemented with kanamycin (50.0 μg/mL). When the culture reached OD_{600} = 0.5, 10.0 mL were transferred to one liter of LB media supplemented with kanamycin (50.0 μg/mL) and grown at 37 °C to an OD_{600} = 0.3. Cultures were transferred to a 16 °C incubator and grown for 60 min before induction with 500.0 μM isopropyl β-D-1-thiogalactopyranoside (IPTG) at OD_{600} = 0.8 and incubated for 20 h. Cells were centrifuged (3000 g, 15 min) and liquid was decanted. Cells were re-suspended in lysis buffer (50.0 mM HEPES, pH 7.4, 150.0 mM KCl, 5.0 mM $MgCl_2$, 5% glycerol, 1.0 mM phenyl methanesulfonyl fluoride (PMSF), 2.0 mM 2-mercaptoethanol). Cells were lysed in a microfluidizer at 12,000 psi. Cobalt resin was washed with water and equilibrated with lysis buffer. Lysate of cells were spun down (11,180 g, 1 h) and the supernatant was incubated with Talon resin for 1 h at 4 °C. The resin was then transferred to a column, the supernatant allowed to flow through and then washed with 1.0 M KCl in lysis buffer. The protein was eluted with imidazole in a step-wise fashion (5.0, 20.0, 100.0, 250.0 mM imidazole in lysis buffer). The protein containing fractions, as confirmed by 12% SDS PAGE, were sealed in 12–14 KDa MWCO dialysis tubing and dialyzed against 4 L dialysis buffer (20.0 mM HEPES, 150.0 mM KCl, 1.0 mM $MgCl_2$) at 4 °C. Dialysates were concentrated in a 30,000 kDa MWCO protein concentrator. Aqueous solution of 50% glycerol was added at an equal volume as dialysate and proteins frozen using liquid nitrogen. All proteins were stored at −80 °C until needed.

3.8. Phosphatase pNPP assay

The *para*-nitro phenol phosphate (*p*NPP) assay was carried out in 96-well transparent plates. Each well contained a 50.0 μL reaction in phosphatase buffer (50.0 mM Tris pH 7.4, 50.0 mM NaCl, 1.0 mM $MgCl_2$, 2.0 mM β-mercaptoethanol) with 1.0 mM pNPP and 250.0–500.0 nM protein. DMSO and 100.0 μM sodium orthovanadate were used as negative and positive controls, respectively.[36] Protein was added to the 96-well plates and incubated with 1.0 μL compound **1** (20.0 μM) or control at 37 °C for 15 min. *p*NPP (1.0 mM) in phosphatase buffer was then added to the plate and incubated for 10 min at 37 °C. Absorbance was measured at 405 nm at 25 °C. Data were exported to Microsoft Excel for analysis. The inhibition percentage was calculated according to the following equation: Inhibition [%] = $100 - (OD_{405}$ compound **1** $- OD_{405}$ DMSO$)/(OD_{405}$ $Na_3VO_4 - OD_{405}$ DMSO$) * 100$.

3.9. Dose-response studies

Dose responses were carried out in phosphatase buffer (as above) using ten-point serial dilution of compound **1** (100.00, 50.00, 25.00, 12.50, 6.25, 3.13, 1.56, 0.78, 0.39 and 0.20 μM). To 96-well transparent plates containing 24.0 μL protein solution (250.0 nM for PTP1B, TCPTP, PTPN3, PTPN5 and PTPN7, 500.0 nM for SHP1 and SHP2), 1.0 μL compound **1** for each of 10 concentrations, DMSO control, and sodium orthovanadate were added. After incubation of the resulting mixture at 37 °C for 15 min, 24.0 μL phosphatase buffer with 2.0 mM *p*NPP was added. The assay plate was incubated for 10 min at 37 °C. Absorbance was measured with a plate reader at 405 nm at 25 °C. Data was exported to Microsoft excel for analysis. Logarithmic regression in KaleidaGraph was used to calculate the IC_{50} values.

Acknowledgements

This work was supported by grants from National Cancer Institute (Grant No. R01 CA090265) and National Institute of General Medical Sciences (Grant No. P41 GM094060). CAPES, Brazil, and China Scholarship Council are thanked for the award of graduate fellowships to J.R.G. and T.S., respectively. We also thank Nicholas C. Massimo for assistance with isolation of the fungus and Ms. Patricia Espinosa-Artiles for her help with culturing of the fungus.

A. Supplementary material

Supplementary data associated with this article can be found, in the online version, at http://dx.doi.org/10.1016/j.bmc.2017.01.048.

References

1. (a) Arnold AE. *Fungal Biol Rev*. 2007;21:51–56; (b) Rodriguez RJ, White JF, Arnold AE, Redman RS. *New Phytol*. 2009;182:314–330.
2. (a) Gunatilaka AAL. *J Nat Prod*. 2006;69:509–526; (b) Kusari S, Spiteller M. *Nat Prod Rep*. 2011;28:1203–1207.
3. Hertweck C. *Nat Chem Biol*. 2009;5:450–452.
4. Cichewicz RH. *Nat Prod Rep*. 2010;27:11–22.
5. (a) Pettit RK. *Appl Microbiol Biotechnol*. 2009;83:19–25; (b) Rateb ME, Hallyburton I, Houssen WE, et al. *RSC Adv*. 2013;3:14444–14450.
6. Pimentel-Elardo SM, Sorensen D, Ho L, et al. *ACS Chem Biol*. 2015;10:2616–2623.
7. (a) Vervoort HC, Drašković M, Crews P. *Org Lett*. 2011;13:410–413; (b) Shwab EK, Bok JW, Tribus M, Galehr J, Graessle S, Keller NP. *Eukaryot Cell*. 2007;6:1656–1664; (c) Henrikson JC, Hoover AR, Joyner PM, Cichewicz RH. *Org Biomol Chem*. 2009;7:435–438; (d) Albright JC, Henke MT, Soukup AA, et al. *ACS Chem Biol*. 2015;10:1535–1541.
8. (a) Fisch KM, Gillaspy AF, Gipson M, et al. *J Ind Microbiol Biotechnol*. 2009;36:1199–1213; (b) Williams RB, Henrikson JC, Hoover AR, Lee AE, Cichewicz RH. *Org Biomol Chem*. 2008;6:1895–1897; (c) Yakasai AA, Davison J, Wasil Z, et al. *J Am Chem Soc*. 2011;133:10990–10998; (d) Beau J, Mahid N, Burda WN, et al. *Mar Drugs*. 2012;10:762–774; (e) Wang X, Filho JGS, Hoover AR, et al. *J Nat Prod*. 2010;73:942–948.
9. VanderMolen KM, Darveaux BA, Chen W-L, Swanson SM, Pearce CJ, Oberlies NH. *RSC Adv*. 2014;4:18329–18335.
10. After this work was completed, a paper describing the isolation and structure elucidation of verruculide B with the same gross structure as **1** appeared in the literature (see ref. 11); however, these authors reported that attempted determination of the absolute stereochemistry of verruculide B proved to be unsuccessful.
11. Yamazaki H, Nakayama W, Takahashi O, et al. *Bioorg Med Chem*. 2015;25:3087–3090.
12. Fuska J, Uhrín D, Proksa B, Voticky Z, Ruppeldt J. *J Antibiot*. 1986;39:1605–1608.
13. Komai S, Hosoe T, Itabashi T, et al. *Heterocycles*. 2005;65:2771–2776.
14. (a) Ui H, Shiomi K, Yamaguchi Y, et al. *J Antibiot*. 2001;54:234–238; (b) Takano D, Nagamitsu T, Ui H, et al. *Tetrahedron Lett*. 2001;42:3017–3020.
15. Sturdikova M, Proksa B, Fuska J, Stancikova M. *Biologia*. 1995;50:233–236.
16. Upadhyay RK, Strobel GA, Coval SJ, Clardy J. *Experientia*. 1990;46:982–984.
17. Fuska J, Fuskova A, Nemec P. *Biologia*. 1979;34:735–739.
18. Xia X-K, Huang H-R, She Z-G, et al. *Helv Chim Acta*. 2007;90:1925–1931.
19. Liu Y, Xia G, Li H, et al. *Planta Med*. 2014;80:912–917.
20. Tautz L, Critton DA, Grotegut S. *Methods Mol Biol*. 2013;1053:179–221.
21. (a) Shibano M, Naito H, Taniguchi M, Wang N-H, Baba K. *Chem Pharm Bull*. 2006;54:717–718; (b) Krohn K, Bahramsari R, Flörke U, et al. *Phytochemistry*. 1997;45:313–320.
22. (a) Di Bari L, Pescitelli G, Pratelli C, Pini D, Salvadori P. *J Org Chem*. 2001;66:4819–4825; (b) Górecki M, Jabłońska E, Kruszewska A, et al. *J Org Chem*. 2007;72:2906–2916; (c) Politi M, De Tommasi N, Pescitelli G, Di Bari L, Morelli I, Braca A. *J Nat Prod*. 2002;65:1742–1745; (d) Tang W-Z, Ma S-G, Yu S-S, Qu J, Liu Y-B, Liu J. *J Nat Prod*. 2009;72:1017–1021.
23. (a) Su BN, Park EJ, Mbwambo ZH, et al. *J Nat Prod*. 2002;65:1278–1282; (b) Seco JM, Quiñoá E, Riguera R. *Chem Rev*. 2004;104:17–118.
24. (a) Alonso A, Sasin J, Bottini N, et al. *Cell*. 2004;117:699–711; (b) Andersen JN, Jansen PG, Echwald SM, et al. *FASEB J*.. 2004;18:8–30; (c) Bialy L, Waldmann H. *Angew Chem Int Ed Engl*. 2005;44:3814.
25. Goldstein BJ. *Curr Drug Targets Immune Endocr Metabol Disord*. 2001;1:265–275.
26. Wiede F, Shields BJ, Chew SH, et al. *J Clin Invest*. 2011;121:4758–4774.
27. Tiganis T. *FEBS J*. 2013;280:445–458.

28. Wu C, Sun M, Liu L, Zhou GW. *Gene*. 2003;306:1–12.
29. Viant C, Fenis A, Chicanne G, Payrastre B, Ugolini S, Vivier E. *Nat Commun*. 2014;5. http://dx.doi.org/10.1038/ncomms6108.
30. Fan L-C, Shiau C-W, Tai W-T, et al. *Oncogene*. 2015;34:5252–5263.
31. U'Ren JM, Lutzoni F, Miadlikowska J, Arnold AE. *Microb Ecol*. 2010;60:340–353.
32. Massimo NC, Devan MMN, Arendt KR, et al. *Microb Ecol*. 2015;70:61–76.
33. Altschul SF, Gish W, Miller W, Myers EW, Lipman DJ. *J Mol Biol*. 1990;215:403–410.
34. Davey ML, Currah RS. *Am J Bot*. 2009;96:1281–1288.
35. Swofford DL. *Phylogenetic analysis using parsimony (∗and other methods), Version 4*. Sunderland, MA: Sinauer Associates; 2002.
36. (a) Martin KR, Narang P, Xu Y, et al. *PLoS ONE*. 2012;7:e50217;
(b) Chen C, Cao M, Zhu S, et al. *Sci Rep*. 2015;5. http://dx.doi.org/10.1038/srep17626.